New Journal of Physics
The open-access journal for physics

Electronic properties of Cs-intercalated single-walled carbon nanotubes derived from nuclear magnetic resonance

E Abou-Hamad[1,2,3], C Goze-Bac[1], F Nitze[2], M Schmid[4], R Aznar[1], M Mehring[4] and T Wågberg[2,5]

[1] nanoNMRI group, UMR5587, Université Montpellier II, Place E Bataillon, 34095 Montpellier Cedex 5, France
[2] Department of Physics, Umeå University, 90187 Umeå, Sweden
[3] KAUST Catalysis Center (KCC), King Abdullah University of Science and Technology, Thuwal, Saudi Arabia
[4] Physikalisches Institut, Universität Stuttgart, D-70569 Stuttgart, Germany
E-mail: Thomas.wagberg@physics.umu.se

New Journal of Physics **13** (2011) 053045 (9pp)
Received 2 March 2011
Published 24 May 2011
Online at http://www.njp.org/
doi:10.1088/1367-2630/13/5/053045

Abstract. We report on the electronic properties of Cs-intercalated single-walled carbon nanotubes (SWNTs). A detailed analysis of the ^{13}C and ^{133}Cs nuclear magnetic resonance (NMR) spectra reveals an increased metallization of the pristine SWNTs under Cs intercalation. The 'metallization' of Cs_xC materials where $x = 0$–0.144 is evidenced from the increased local electronic density of states (DOS) $n(E_F)$ at the Fermi level of the SWNTs as determined from spin–lattice relaxation measurements. In particular, there are two distinct electronic phases called α and β and the transition between these occurs around $x = 0.05$. The electronic DOS at the Fermi level increases monotonically at low intercalation levels $x < 0.05$ (α-phase), whereas it reaches a plateau in the range $0.05 \leqslant x \leqslant 0.143$ at high intercalation levels (β-phase). The new β-phase is accompanied by a hybridization of Cs(6s) orbitals with C(sp^2) orbitals of the SWNTs. In both phases, two types of metallic nanotubes are found with a low and a high local $n(E_F)$, corresponding to different local electronic band structures of the SWNTs.

[5] Author to whom any correspondence should be addressed.

The electronic properties of single-walled carbon nanotubes (SWNTs) have attracted a great deal of interest in the last decade. Non-intercalated SWNTs have been shown both theoretically [1, 2] and experimentally [3] to exhibit either metallic or semi-conducting properties depending on their chirality and diameter. Tuning the electronic density of states (DOS) is of paramount scientific and technological interest. One of the ways to proceed is to intercalate nanotubes with alkali metals, which is known to change the electronic properties of the nanotubes due to electron transfer from the alkali atoms to the nanotubes. Despite the progress made in the last decade, there are still many open questions concerning this transfer. A specific question concerning the charge transfer is if under some conditions the alkali metal does not fully transfer its valence electrons to the nanotube carbons [4, 5]. In this systematic intercalation study, we have applied ^{13}C and ^{133}Cs nuclear magnetic resonance (NMR) to investigate seven samples of ^{13}C-enriched (10%) Cs-doped SWNTs (Cs_xC, $x = 0$–0.143). We show that doped SWNTs exhibit two distinct electronic phases called α and β and that the transition between these phases occurs around $x = 0.05$. The electronic DOS, $n(E_F)$, at the Fermi level increases monotonically at low intercalation level $x < 0.05$ (α-phase), whereas it reaches a plateau in the range $0.05 \leqslant x \leqslant 0.143$ at high intercalation level (β-phase). We present strong evidence that this new β-phase is accompanied by a hybridization of Cs(6s) orbitals with the C(sp^2) orbitals of the SWNTs.

Raw SWNT samples were synthesized by arc-discharge using Pt and Rh as catalysts as described in [6]. The SWNTs had an average diameter of 1.4 ± 0.2 nm and a bundle length of several micrometers [7, 8]. All SWNTs were ^{13}C isotope enriched to 10% in order to increase the signal-to-noise ratio in the same way as previously reported by Ruemelli *et al* [9]. The preparation of Cs-intercalated SWNTs proceeded by saturating SWNTs by Cs vapor-transport onto degassed SWNT at 200 °C in a cycled process for 10 days. Theoretical and experimental studies have shown that the intercalation of SWNT saturates at a stoichiometry of approximately $Cs_{0.14}C$ [10–12]. The enriched saturated sample was then mixed in different ratios with the pristine SWNT sample by a Schlenk-like method. All samples were treated under secondary vacuum. Before the samples were mixed and annealed at 300 °C for 2 weeks the mixtures were analyzed with static NMR. The different line shapes of the pristine and saturated intercalated SWNTs reflecting the difference in chemical and Knight shift anisotropy is clear from figure 1(a). By extracting the contribution of the two different line shapes (pristine and saturated) in the different mixtures before annealing, the ratio of non-intercalated SWNTs and saturated intercalated SWNTs could be estimated. After the heat treatment the samples were again controlled by static NMR. The change in line shape of the samples (figure 1(b)) confirms the homogeneity of the samples with stoichiometries Cs_xC ($x = 0.028$–0.14) (errors $\approx$ 4–8%).

^{13}C NMR experiments were performed on Bruker and Tecmag Apollo NMR solid state spectrometers at a magnetic field of 4.7 T and a Larmor frequency of 50.3 MHz. Static NMR spectra were obtained in the temperature range of 5–300 K. ^{13}C NMR line shifts are referred to tetramethylsilane (TMS). ^{133}Cs NMR measurement were carried out on a home-built pulsed NMR spectrometer equipped with a sweep magnet working at 9.1 T and a Larmor frequency of 50.7 MHz. ^{133}Cs NMR line shifts are referred to an aqueous solution of 1 M $CsNO_3$. ^{13}C spin–lattice relaxations were obtained using a saturation recovery pulse technique and a Hahn echo as the detection sequence.

Figure 1(b) displays the static ^{13}C-NMR spectra of pristine and Cs-intercalated SWNTs. The spectrum of pristine SWNTs shows a characteristic sp^2 powder line shape in agreement with earlier studies [8]. However, already at low intercalation levels, $x = 0.028$–0.038, the

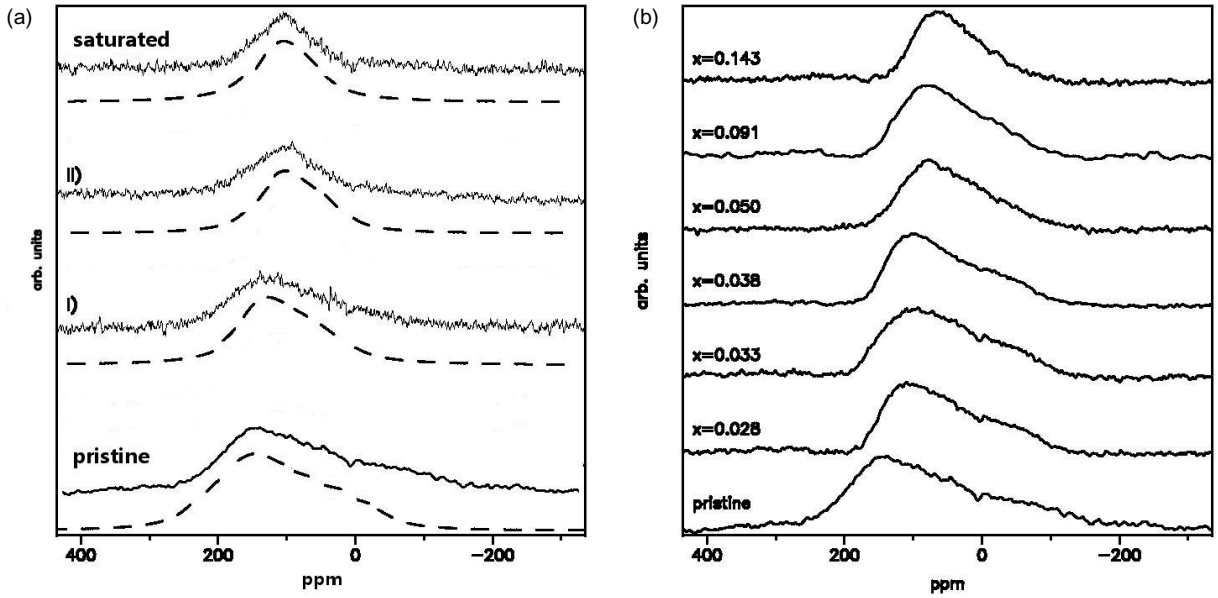

Figure 1. (a) Static ^{13}C NMR spectra at room temperature before annealing. 'Pristine': pristine SWNTs; 'I)' and 'II)': mixture of saturated $Cs_{0.14}C$ and pristine SWNTs; and 'Saturated': saturated $Cs_{0.14}C$. Fitted tensors are shown to explain how the doping ratio was established. Spectra I and II were fitted with both types of tensors (giving a doping ratio of 0.033 ± 0.003 and 0.091 ± 0.005, respectively). The fits were performed by following the procedure described in [8, 18]. (b) Static ^{13}C NMR spectra at room temperature after annealing the samples at 300 °C for 2 weeks. Spectra show pristine SWNTs and Cs_xC intercalated SWNTs for different intercalation levels x increasing from the bottom to the top as indicated in the figure.

NMR spectra exhibit a clear anisotropy reduction of about 200 ppm due to a change into a more metallic-like shift anisotropy as reported by Latil *et al* [13]. All samples show a similar and strong further narrowing of the line shape when the intercalation level is increased from $x = 0.05$ to 0.14, indicating that the samples exhibit an increasing trend in metallic behavior.

There are two known contributions to the total ^{13}C NMR shift of doped SWNTs, namely the Knight shift K and the chemical shift σ, where the Knight shift arises from the hyperfine coupling of the nuclei to conduction electron spins and the chemical shift summarizes all contributions from orbital currents due to local magnetic fields. Both Knight shift K and T_1 relaxation are affected by the DOS at the Fermi surface $n(E_F)$ if shift and relaxation are dominated by the magnetic interaction with the conduction electrons of the metal [14]. In carbon nanotubes as well as in fullerenes and other anisotropic and complex conducting materials the simple classical relations applied to classical metals do not hold. Instead, the anisotropy of the hyperfine interaction as well as non-classical electrodynamics need to be considered. It is beyond the scope of this paper to review these theoretical aspects. We therefore just refer to the results of earlier publications [15–17]. A review of these topics can be found in [18, 19].

The relaxation rate can be expressed as

$$\frac{1}{T_1 T} = \pi k_B \hbar a^2 \left(1 + \frac{1}{2}\varepsilon\right) n\,(E_F)^2\,, \tag{1}$$

where $a = A_{iso} = 5.8 \times 10^7\ s^{-1}$ is the isotropic hyperfine interaction, $\varepsilon = d^2/a^2$, $d/a = 2 \times A_{dip}/A_{iso} = 3.9$, is the anisotropy parameter with dipolar contribution d corresponding to the anisotropic but axially symmetric hyperfine interaction and the other symbols have their usual meaning. The values of $A_{iso} = 5.8 \times 10^7\ s^{-1}$ and $A_{dip} = 1.1 \times 10^7\ s^{-1}$ leading to the value of $\varepsilon = 3.9$ are derived from the work of Pennington and Stenger [18] for sp^2-bonded carbon materials.

There is a compact notation of the relation between the isotropic Knight shift and the relaxation time as [17]

$$T_1 T K_{iso}^2 \left(1+\frac{1}{2}\varepsilon\right) C_0 S_K = 1, \tag{2}$$

with

$$C_0 = 4\pi \frac{k_B}{\hbar} \left(\frac{\gamma_n}{\gamma_e}\right)^2$$

and $S_K = 1$ for uncorrelated electrons as considered here. In this communication we evaluate only the relaxation rate $1/T_1$ and its proportionality to $n(E_F)^2$, a technique that has been shown to be appropriate to estimate $n(E_F)$ [20–23].

The observed relaxation curves signal a two-component model with one slow relaxing and one fast relaxing component, which can be rationalized by the two types of SWNTs to be discussed in the following. The magnetization recovery, $M(t)$, was correspondingly fitted with a double exponential function of the type (inset of figure 2(a) at room temperature)

$$M = M_s(1 - e^{-t/T_{1s}}) + M_m(1 - e^{-t/T_{1m}}), \tag{3}$$

where M_s and M_m are the equilibrium magnetizations for the two components. T_{1s} and T_{1m} are the two different T_1 relaxation times for the two components. The relative magnitudes, M_s/M_0 and M_m/M_0, with $M_0 = M_s + M_m$ do not differ in a systematic way for the different stoichiometries, and are determined to be $60\% \pm 7\%$ and $40\% \pm 7\%$. The errors of the T_{1s} and T_{1m} values vary around 10% for different temperatures.

For the pristine SWNTs, the slow and the fast relaxing components derived from the fit at room temperature result in $T_{1s} = 75$ s and $T_{1m} = 2$ s and were assigned to semiconducting and metallic tubes, respectively [8, 22]. The two components of SWNT samples are also in agreement with recent high-resolution NMR experiments [24]. On doping we observe a decrease of both relaxation times, T_{1s} and T_{1m}, as expected due to the increase of the DOS of both the metallic and semiconducting tubes. They reach comparable values to the one for the pristine metallic SWNT (e.g. $Cs_{0.028}C$ $T_{1s} = 9$ s and $T_{1m} = 1.3$ s). With increased intercalation, both relaxation rates $1/T_{1s}$ and $1/T_{1m}$ increase until they 'saturate' ($T_{1s} = 2.2$ s and $T_{1m} = 0.25$ s) for samples with $x = 0.05$–0.14. In our case, we assign the two components to two kinds of metallic tubes (α_l- and α_h-type) obtained by doping the originally semiconducting and metallic SWNTs. Recent NMR studies on pristine SWNTs [25] and double-walled carbon nanotubes (DWNTs) [23, 26] have used partly different models based on a stretched distribution of T_1 values around *one* average. In studies of the DWNTs this is rationalized by a purely metallic state of the inner tubes in the DWNTs according to the authors. For all our samples with different doping levels *two* components of T_1 values are present. It should, however, be noted that the two-component model adopted here is a simplified picture that enables us to estimate the DOS of the SWNTs. In a more complicated view, the heterogeneity of the SWNTs would require one

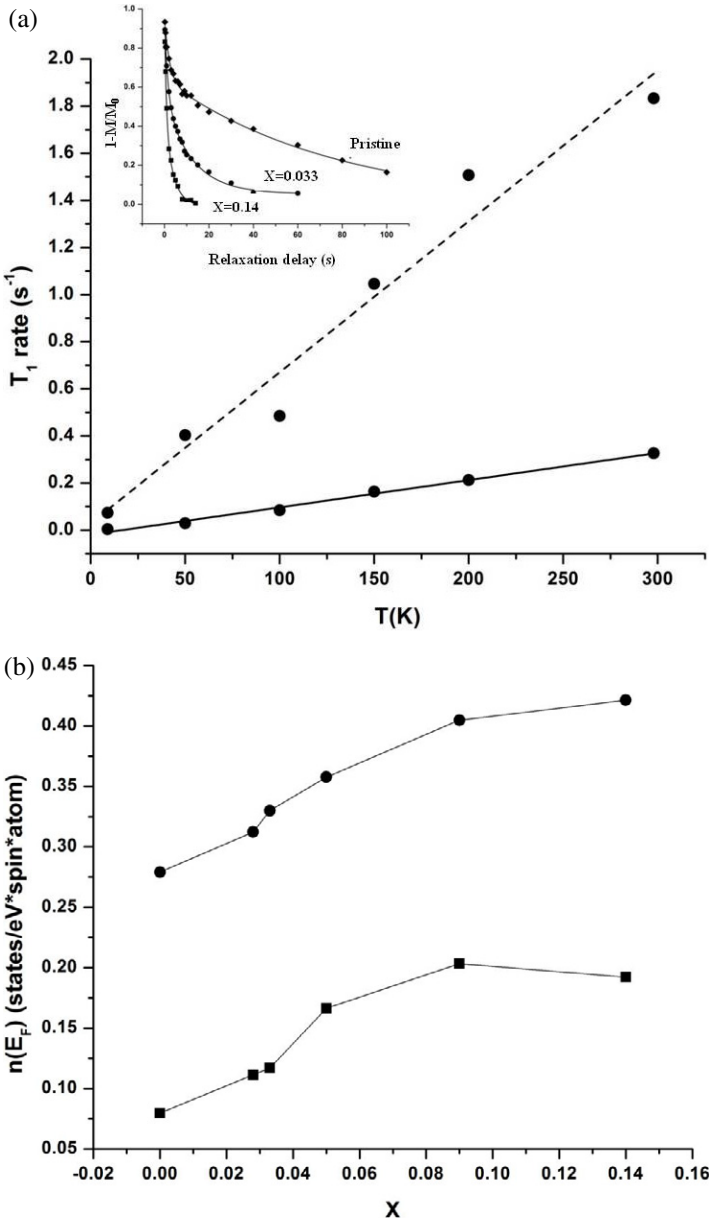

Figure 2. (a) Temperature-dependent ^{13}C NMR spin–lattice relaxation rates plotted as $1/T_1$ against temperature T for the sample $Cs_{0.14}C$. The linear relation shows good agreement with Korringha law behavior; the inset shows ^{13}C NMR magnetization recovery at room temperature plotted as $1-(M/M_0)$ obtained by fitting double exponential functions (equation (3)), for pristine SWNT (diamonds), $Cs_{0.028}C$ (squares) and $Cs_{0.14}C$ (circles). (b) Local DOS at the Fermi level of the SWNTs as a function of x for Cs_xC; squares show low-DOS-type tubes (60%) and circles show high-DOS-type tubes (40%). The connecting lines are a guide to the eyes.

to use a distribution of T_1 values around T_{1s} and T_{1m}. The previous use of the two-component model in similar studies [8, 22] and regarding T_{1s} and T_{1m} as representing the average values of the two distributions in our opinion justifies the use of the simplified model.

Using equation (1) that takes into account both isotropic and anisotropic hyperfine interactions in contrast to earlier studies of non-intercalated SWNTs [8, 22] and doped C_{60} [27, 28], we can determine the DOS at the Fermi level, $n(E_F)$, for our samples (figure 2(b)). As a direct consequence of the Korringa law (figure 2(a)) the two types of tubes with long and short relaxation times are calculated to have a 'low' DOS (α_l-type tubes, 60%) or a high DOS (α_h-type tubes, 40%), respectively. The values of $n(E_F)$ were derived using the relaxation times determined at room temperature (figure 2). Low-temperature data, however, support well the derived values shown in figure 2(b). Our derived value for $n(E_F)$ is significantly higher than the corresponding value for non-intercalated tubes in the paper by Tang *et al* [22] but with a very similar DOS ratio between the high- and low-DOS tubes. Referring to the discussion above about the necessity of taking also anisotropic hyperfine interactions into account for carbon nanotubes, we do believe that our derived values are more realistic but that the absolute values of $n(E_F)$ largely depend on the parameters a and d.

Note that $n(E_F)$ does not follow a simple linear dependence but increases steadily to an intercalation level corresponding to $x = 0.05$ where it starts to flatten out. This is especially clear for tubes with a low DOS. Our observations are in excellent agreement with Kazaoui *et al* [29] and Grigorian *et al* [30] who observed a maximum in the conductivity of Cs-intercalated SWNTs for similar intercalation levels. The behavior of the DOS observed here as well as the conduction plateau observed by Kazaoui *et al* [29] and Grigorian *et al* [30] could indicate a different charge transfer behavior of Cs atoms added in the high intercalation regime. To further explore this charge transfer behavior, we have performed ^{133}Cs NMR experiments as shown in figure 3. At low intercalation levels, a single quadrupolar broadened line located at 0 ppm is observed which we assign to Cs(α). At higher intercalation levels above $x = 0.038$, a second line located around 2700 ppm appears and is assigned to a different type of Cs ion denoted Cs(β) which increases progressively with Cs concentration.

The Cs(α) line position around 0 ppm is a signature of almost fully ionized Cs^{+1} cations (Cs^0 metal is found at 14600 ppm), whereas the strong paramagnetic shift of the Cs(β) line indicates the presence of $Cs^{+\delta}$ cations with approximately $\delta = 1 - (2700/14600) = 0.82$, which signals some hybridization with the carbon orbitals [31]. The two lines at high Cs concentration may be explained by the existence of two non-equivalent Cs adsorption sites in the SWNT bundle as proposed by Bendiab *et al* [32] and Bantignies *et al* [33]. Here we favor, however, two different intercalation phases, namely the α-phase corresponding to Cs(α) and the β-phase corresponding to Cs(β) in comparison to the stage I Cs–GIC compound CsC_8 [30]. We point out, however, that both these phases contain two types of tubes as revealed by the relaxation experiments.

A two-phase model for intercalated SWNTs has been discussed in several reports [4, 30, 32–36] and our results are in excellent agreement with *in situ* conductivity and Raman studies on Rb-intercalated SWNTs [35, 36].

The paramagnetically shifted Cs(β) line implies a strong hyperfine coupling between Cs nuclei and the conduction electrons of the carbon nanotubes arising from the strong Fermi contact-like electrons–nuclear interaction with the hybridized Cs(6s)–C(sp^2) orbitals. This is supported by a strong Korringa-like relaxation of the Cs(β) line (not shown here). Moreover, a well-developed quadrupolar interaction of Cs(β) that does not vanish at higher temperatures suggests a rather rigid bonding of Cs(β) in contrast to Cs(α) that show large mobility at higher temperatures.

A limited charge transfer was also proposed by Lu *et al* [4] who found a charge transfer limitation in K-intercalated nanotubes theoretically. Above a stoichiometry of $K_{0.037}C$, the

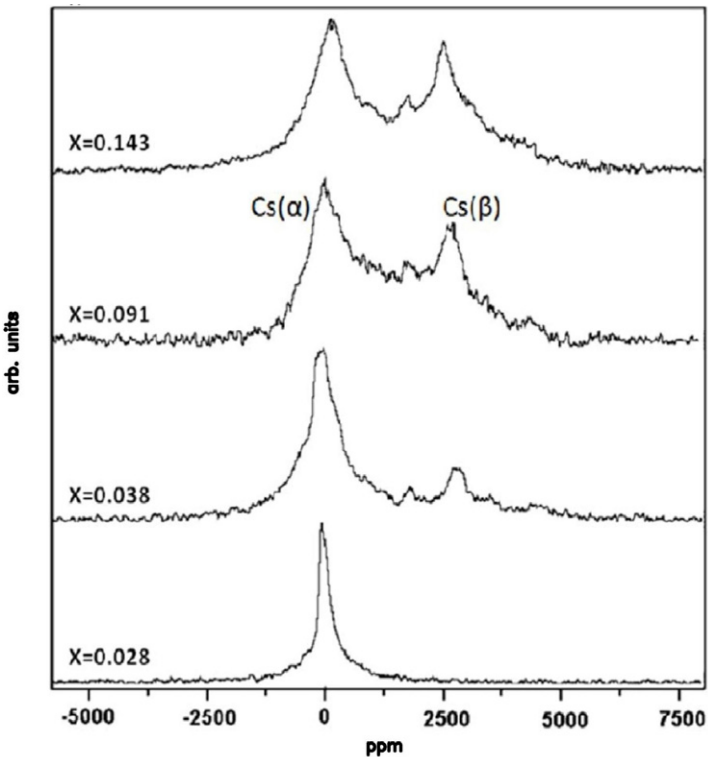

Figure 3. (a) ^{133}Cs NMR spectra of Cs_xC for different intercalation levels x. (b) ^{13}C MAS NMR spectra of CsC_x. Stars represent spinning sidebands. Spinning rate $\omega = 10$ kHz for pristine SWNT and $\omega = 4$ kHz for doped SWNT with a repetition time of $\tau = 30$ s. (b) ^{133}Cs NMR spectra of CsC_x.

authors claim a preferential hybridization between K (4s) orbital and nearly free electron states of the nanotube, leading to a limit in charge transfer. Such hybridization was also proposed theoretically by Miyake and Saito [5]. Their calculated effect is expected to be even more significant for Cs(β) due to the higher hybridization affinity of cesium. This might in fact explain our observation of the plateau in the DOS $n(F_F)$ of carbon nanotubes in the region from $Cs_{0.05}C$ to $Cs_{0.14}C$ as well as the conductivity plateau observed by Kazaoui *et al* [29].

We have shown that intercalated SWNTs have a complex metallic ground state, which is tunable by the Cs content. The T_1-rates of all samples follow a linear relation in agreement with Korringa's law. At low intercalation levels the local electronic DOS at the Fermi level increases consistently up to $x = 0.05$ but flattens out for higher intercalation levels. At high intercalation levels the spectra indicate a transition into a two-phase intercalation model, which we label as α- and β-phase. Static ^{133}Cs NMR measurements affirm this model and show that at high intercalation levels a certain fraction of the Cs atoms does not take part in the full charge transfer to the SWNT carbons but instead leads to a hybridization between the valence electrons of the Cs atoms and the valence electrons of the nanotubes.

Our study confirms and explains several recent theoretical and experimental studies on alkali-metal-intercalated carbon nanotubes. This study proves the versatility of NMR to extract significant information on the metallic and local properties of intercalated carbon nanotubes. Moreover, this study provides important additional knowledge about the variety of electronic states of carbon nanotubes, which is of significant importance for future applications of SWNTs.

Acknowledgments

TW thanks the Wenner-Gren Foundation, the Magnus Bergvalls Foundation and the Swedish Research Council for support (dnr: 2010-3973). CGB is grateful to the Région Languedoc-Roussillion for financial support.

References

[1] Mintmire J W, Dunlap B I and White C T 1992 Are fullerene tubules metallic? *Phys. Rev. Lett.* **68** 631
[2] Saito R, Fujita M, Dresselhaus G and Dresselhaus M S 1992 Electronic structure of chiral graphene tubules *Appl. Phys. Lett.* **60** 2204
[3] Wildoer J G W, Venerna L C, Rinzler A G, Smalley R E and Dekker C 1998 Electronic structure of atomically resolved carbon nanotubes *Nature* **391** 59
[4] Lu L, Nagase S, Zhang S and Peng L 2004 Energetic, geometric, and electronic evolutions of K-doped single-wall carbon nanotube ropes with K intercalation concentration *Phys. Rev.* B **69** 205304
[5] Miyake T and Saito S 2002 Electronic structure of potassium-doped carbon nanotubes *Phys. Rev.* B **65** 165419
[6] Journet C, Maser W K, Bernier P, Loiseau A, Lamyde la, Chapelle M, Lefrant S, Deniard P, Leek R and Fischer J E 1997 Large-scale production of single-walled carbon nanotubes by the electric-arc technique *Nature* **388** 756
[7] Goze-Bac C *et al* 2001 ^{13}C NMR evidence for dynamics of nanotubes in ropes *Phys. Rev.* B **63** 100302
[8] Goze-Bac C, Latil S, Lauginie P, Jourdain V, Conard J, Duclaux L, Rubio A and Bernier P 2002 Magnetic interactions in carbon nanostructures *Carbon* **40** 1825
[9] Rümmeli M H *et al* 2007 Isotope-engineered single-wall carbon nanotubes; a key material for magnetic studies *J. Phys. Chem.* C **111** 4094
[10] Dresselhaus M S and Dresselhaus G 1981 Intercalation compounds of graphite *Adv. Phys.* **30** 139
[11] Carver G P 1970 Nuclear magnetic resonance in cesium–graphite intercalation compounds *Phys. Rev.* B **2** 2284
[12] Suzuki S, Bower C and Zhou O 1998 *In-situ* TEM and EELS studies of alkali-metal intercalation with single-walled carbon nanotubes *Chem. Phys. Lett* **285** 230
[13] Latil S, Henrard L, Goze-Bac C, Bernier P and Rubio A 2001 ^{13}C NMR chemical shift of single-wall carbon nanotubes *Phys. Rev. Lett.* **86** 3160
[14] Yazyev O V and Helm L 2005 Isotropic Knight shift of metallic carbon nanotubes *Phys. Rev.* B **72** 245416
[15] Mehring M 1987 Electron transport in (FA)2_x-type organic conductors *Low Dimensional Conductors and Superconductors* ed D Jerome and L G Caron (New York: Plenum) p 185
[16] Mehring M 1992 What does NMR tell us about the electronic state of high-T_c superconductors? *Appl. Magn. Reson.* **3** 383
[17] Mehring M, Rachdi F and Zimmer G 1994 Analysis of the C-13 Knight-shift and spin–lattice relaxation in A3C60 (A = Rb or K) *Phil. Mag.* **B** 70787
[18] Pennington C H and Stenger V A 1996 Nuclear magnetic resonance of C60 and fulleride superconductors *Rev. Mod. Phys.* **68** 856
[19] Zurek E and Autschbach J 2009 NMR computations for carbon nanotubes from first principles: present status and future directions *Int. J. Quantum Chem.* **109** 3343
[20] Schmid M, Goze-Bac C, Krämer S, Roth S, Mehring M, Mathis C and Petit P 2006 Metallic properties of Li-intercalated carbon nanotubes investigated by NMR *Phys. Rev.* B **74** 073416
[21] Abragam A 1986 *Principles of Nuclear Magnetism* (Oxford: Oxford University Press)
[22] Tang X-P, Kleinhammes A, Shimoda H, Fleming L, Bennoune K Y, Sinha S, Bower C, Zhou O and Wu Y 2000 Electronic structures of single-walled carbon nanotubes determined by NMR *Science* **288** 492
[23] Singer P M, Wzietek P, Alloul H, Simon F and Kuzmany H 2005 NMR evidence for gapped spin excitations in metallic carbon nanotubes *Phys. Rev. Lett.* **95** 236403

[24] Engtrakul C, Davis M F, Mistry K, Larsen B A, Dillon A C, Heben M J and Blackburn J L 2010 Solid-state ^{13}C NMR assignment of carbon resonances on metallic and semiconducting single-walled carbon nanotubes *J. Am. Chem. Soc.* **132** 9956

[25] Ihara Y, Wzietek P, Alloul H, Rummeli M H, Pichler Th and Simon F 2010 Incidence of the Tomonaga-Luttinger liquid state on the NMR spin–lattice relaxation in carbon nanotubes *Europhys. Lett.* **90** 17004

[26] Dora B, Gulacsi M, Simon F and Kuzmany H 2007 Spin gap and Luttinger liquid description of the NMR relaxation in carbon nanotubes *Phys. Rev. Lett.* **99** 166402

[27] Antropov V P, Mazin I I, Andersen O K, Liechtenstein A I and Jepsen O 1993 Dominance of the spin-dipolar NMR relaxation mechanism in fullerene superconductors *Phys. Rev.* B **47** R12373

[28] Tycko R, Dabbagh G, Rosseinsky M J, Murphy D W, Fleming R M, Ramirez A P and Tully J C 1991 ^{13}C NMR spectroscopy of K_xC_{60}: phase separation, molecular dynamics, and metallic properties *Science* **253** 884

[29] Kazaoui S, Minami N, Jacquemin R, Kataura H and Achiba Y 1999 Amphoteric doping of single-wall carbon-nanotube thin films as probed by optical absorption spectroscopy *Phys. Rev.* B **60** 13339

[30] Grigorian L, Sumanasekera G U, Loper A L, Fang S, Allen J L and Eklund P C 1998 Transport properties of alkali-metal-doped single-wall carbon nanotubes *Phys. Rev.* B **58** 4195

[31] Estrade-Szwarckopf H, Conrad J, Lauginie P, Klink J, Guerard D and Lagrange P 1981 ^{133}Cs NMR studies of cesium GIC *Physics of Intercalation Compounds (Series in Solid State Sciences* vol 38*)* (Berlin: Springer) p 274

[32] Bendiab N, Saitta A M, Aznar R, Sauvajol J L, Almairac R, Mirebeau I and Andre G 2008 Rubidium localization in single-walled carbon nanotube bundles: structural study *Phys. Rev.* B **78** 104108

[33] Bantignies J L, Alvarez L, Aznar R, Almairac R, Sauvajol J L, Duclaux L and Villain F 2005 EXAFS study of rubidium-doped single-wall carbon nanotube bundles *Phys. Rev.* B **71** 195419

[34] Akdim B, Duan X, Shiffler D A and Pachter R 2005 Theoretical study of the effects of alkali-metal atoms adsorption on Raman spectra of single-wall carbon nanotubes *Phys. Rev.* B **72** 121402

[35] Chen G, Furtado C A, Bandow S, Iijima S and Eklund P C 2005 Anomalous contraction of the C–C bond length in semiconducting carbon nanotubes observed during Cs doping *Phys. Rev.* B **71** 045408

[36] Bendiab N, Spina L, Zahab A, Poncharal P, Marliére C, Bantignies J L, Anglaret E and Sauvajol J L 2001 Combined *in situ* conductivity and Raman studies of rubidium doping of single-wall carbon nanotubes *Phys. Rev.* B **63** 153407